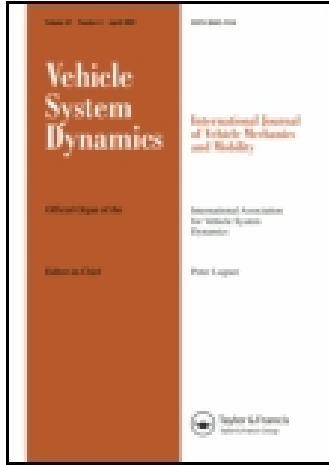


This article was downloaded by: [Florida Atlantic University]

On: 22 November 2014, At: 17:05

Publisher: Taylor & Francis

Informa Ltd Registered in England and Wales Registered Number: 1072954 Registered office: Mortimer House, 37-41 Mortimer Street, London W1T 3JH, UK



## Vehicle System Dynamics: International Journal of Vehicle Mechanics and Mobility

Publication details, including instructions for authors and subscription information:

<http://www.tandfonline.com/loi/nvsvd20>

### Vehicle Following Control in Lateral Direction for Platooning

Takehiko Fujioka<sup>a</sup> & Manabu omae<sup>a</sup>

<sup>a</sup> Department of Mechanical Engineering , Takehiko Fujioka and Manabu Omae.

The University of Tokyo , 7-3-1 Hongo, Bunkyo-ku, Tokyo, 113, JAPAN Phone: TEL

+81-3-3812-2111 Fax: TEL +81-3-3812-2111 E-mail:

Published online: 27 Jul 2007.

To cite this article: Takehiko Fujioka & Manabu omae (1998) Vehicle Following Control in Lateral Direction for Platooning, Vehicle System Dynamics: International Journal of Vehicle Mechanics and Mobility, 29:S1, 422-437, DOI: [10.1080/00423119808969576](https://doi.org/10.1080/00423119808969576)

To link to this article: <http://dx.doi.org/10.1080/00423119808969576>

PLEASE SCROLL DOWN FOR ARTICLE

Taylor & Francis makes every effort to ensure the accuracy of all the information (the "Content") contained in the publications on our platform. However, Taylor & Francis, our agents, and our licensors make no representations or warranties whatsoever as to the accuracy, completeness, or suitability for any purpose of the Content. Any opinions and views expressed in this publication are the opinions and views of the authors, and are not the views of or endorsed by Taylor & Francis. The accuracy of the Content should not be relied upon and should be independently verified with primary sources of information. Taylor and Francis shall not be liable for any losses, actions, claims, proceedings, demands, costs, expenses, damages, and other liabilities whatsoever or howsoever caused arising directly or indirectly in connection with, in relation to or arising out of the use of the Content.

This article may be used for research, teaching, and private study purposes. Any substantial or systematic reproduction, redistribution, reselling, loan, sub-licensing, systematic supply, or distribution in any form to anyone is expressly forbidden. Terms & Conditions of access and use can be found at <http://www.tandfonline.com/page/terms-and-conditions>

## Vehicle Following Control in Lateral Direction for Platooning

Takehiko Fujioka and Manabu Omae

Department of Mechanical Engineering, The University of Tokyo

7-3-1 Hongo, Bunkyo-ku, Tokyo, 113, JAPAN

TEL +81-3-3812-2111 FAX +81-3-3818-0835

E-mail [fujioka@mech.t.u-tokyo.ac.jp](mailto:fujioka@mech.t.u-tokyo.ac.jp) [omae@vdl.t.u-tokyo.ac.jp](mailto:omae@vdl.t.u-tokyo.ac.jp)

### SUMMARY

Simulation and experimental study on lateral control for autonomous driving is presented in this paper. The objective of the lateral control system is to make the controlled vehicle follow the preceding vehicle. Simulation study is conducted for investigating the relationship between information for lateral control and the tracking accuracy obtained based on the information. Simulation results of vehicle-following control based on five kinds of control algorithms, each of which is designed using some information for lateral control, are compared and discussed. Experimental study is carried out by use of two vehicles to validate results of the simulation study. By both studies, it is clarified that side slip angle is the essential information for implementing an accurate vehicle-following control.

### 1 INTRODUCTION

This paper investigates lateral control for the platooning. The platooning is a method of autonomous driving control where the constituents of a group of vehicles follow the lead vehicle of the group. In the field of studies on control for the platooning, while a lot of studies have been reported on longitudinal control with respect to the relative position of the preceding vehicle, few have been reported on lateral control[1]-[4]. For lateral control, most of studies are concerned with designing a controller with respect to the relative position of the desired path on the road[5]-[16]. In this paper, lateral control with respect to the relative position of the preceding vehicle is focused on.

Methods of lateral control for the platooning can be classified as the road-following method or the vehicle-following method which is adopted in this research. With the vehicle-following method, a vehicle is controlled in order to follow the preceding vehicle detected, see Figure 1. This method has an advantage over the road-following method in requiring no infrastructure on the road. On the other hand, this method requires precise lateral control because of the accumulation of tracking errors, when it is applied to a group of many vehicles. Furthermore, the lateral control must be robust to the influence of a change of a space between the controlled vehicle and the preceding vehicle as well as of a change of a speed of the controlled vehicle.

This study consists of simulation study and experimental study. The simulation study is conducted for the purpose of clarifying the relationship between information for lateral control and the tracking accuracy. The knowledge of necessary information for implementing vehicle-following control with the desired accuracy will make a design of systems easier and more effective. In this study, five kinds of algorithms are investigated. Each of algorithms is designed based on a different combination of information about vehicle parameters and state variables of vehicle dynamics. Vehicle-following simulations are conducted under the condition that a speed and a space are constant, that a speed or a space is changing, and that

simulated vehicle parameters are different from those assumed in the control algorithms. The tracking accuracy based on each of the algorithms is compared and discussed.

Experimental study using two vehicles is carried out to confirm the validity of the result of simulation study. A scanning laser radar installed on the controlled vehicle is utilized for detecting the relative position of the preceding vehicle with respect to the controlled vehicle. The steering angle of the following vehicle is controlled with a steering actuator based on one of the algorithms investigated in the simulation study. Road test is conducted at a speed of 5[m/s], 10[m/s], 15[m/s] and 20[m/s]. Characteristics of step responses and tracking accuracy at a circling maneuver are investigated.

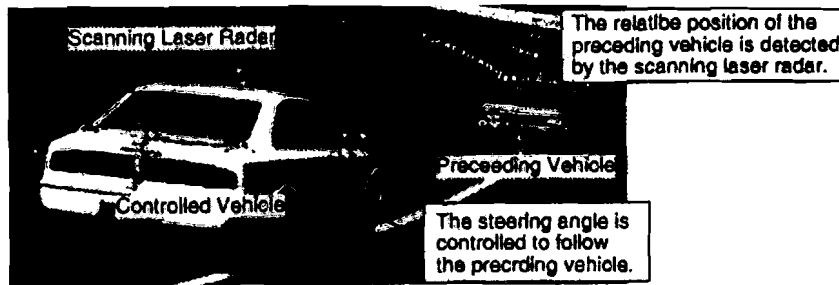


Fig.1 Vehicle-following method

## 2 SIMULATION STUDY

In this chapter, five control algorithms are explained and simulation results based on the algorithms are discussed. The objective of the algorithms is to determine a front steering angle of the controlled vehicle to track a trajectory of the preceding vehicle. The algorithms are so designed that they might be robust to the influence of a change of a vehicle speed and of a change of a space between the two vehicles.

### 2.1 Control Algorithms

Table 1 shows information for lateral control used in each of the algorithms. The relative position of the center of gravity(CG) of the preceding vehicle with respect to the controlled vehicle is assumed to be accurately detected and is utilized for each of the algorithms. In the following subsections, each of the algorithms is explained.

Table 1 Classification of the information for the control algorithms

| algorithm                                      | 1 | 2 | 3 | 4 | 5 |
|--|---|---|---|---|---|
| <b>parameters</b>                              |   |   |   |   |   |
| mass ( $m$ )                                   | — | — | — | ○ | ○ |
| moment of yaw inertia ( $I$ )                  | — | — | — | ○ | ○ |
| distance between CG and front axle ( $l_f$ )   | — | — | — | ○ | ○ |
| distance between CG and rear axle ( $l_r$ )    | — | — | — | ○ | ○ |
| total cornering power of front tires ( $K_f$ ) | — | — | — | ○ | ○ |
| total cornering power of rear tires ( $K_r$ )  | — | — | — | ○ | ○ |
| wheel base ( $l$ )                             | ○ | — | — | ○ | ○ |
| <b>state variables</b>                         |   |   |   |   |   |
| velocity ( $V$ )                               | — | ○ | ○ | ○ | ○ |
| acceleration ( $a$ )                           | — | — | ○ | — | ○ |
| yaw rate ( $\dot{\gamma}$ )                    | — | ○ | ○ | — | ○ |
| side slip angle of CG ( $\beta$ )              | — | — | ○ | — | ○ |

○ required for the algorithm — not required for the algorithm

### 2.1.1 Algorithm 1

Algorithm 1 determines a steering angle according to the geometric relation among positions of front and rear tires of the controlled vehicle and a position of the preceding vehicle. This algorithm requires only information of wheel base of the controlled vehicle. Assuming that tires do not slip, directions of velocity at the positions of the front tire and rear tire are equal to directions of each tire, respectively, where trajectory radius of circling is  $\delta/l$ . The steering angle is derived from the assumption described above.

Figure 2 shows the variables used for the algorithm. The following equation is given by the assumption:

$$\frac{l}{R} = \frac{\delta}{l},$$

where  $R$  denotes a radius of the circle which goes through these three points, positions of centers of front and rear axles of the controlled vehicle, and CG of the preceding vehicle. The steering angle is determined as

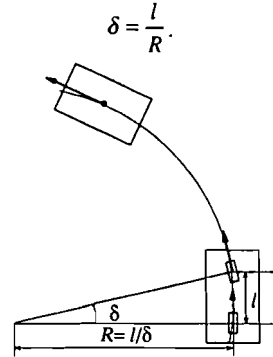


Fig. 2 Algorithm 1

### 2.2.2 Algorithm 2

Algorithm 2 derives a steering angle from a future lateral deviation of a future position of the controlled vehicle from a present position of the preceding vehicle. The future position of the controlled vehicle is estimated using velocity and yaw rate of the controlled vehicle. This algorithm requires the information of state variables of vehicle dynamics that are easy to measure. The steering angle is determined by multiplying a gain not by the future deviation but by the change of yaw rate of the controlled vehicle. The change of yaw rate has the value required to reduce the future deviation to zero. By means of this method, the tracking performance is less affected by a change of a vehicle speed and a change of a space between the two vehicles.

Figure 3 shows the variables used for the algorithm. The time required for the controlled vehicle to reach a detected position of the preceding vehicle is given as

$$t_p = \frac{D}{V},$$

where  $D$  denotes a space, that is, a distance between the controlled vehicle and the preceding vehicle. Assuming that the controlled vehicle travels at a constant yaw rate, estimated lateral displacement in  $t_p$  [s] is given by

$$y_p = D \cdot \frac{1}{2} \gamma \cdot t_p.$$

On the other hand, a relative lateral displacement of the preceding vehicle with respect to the controlled vehicle is given by

$$y_{car1} = D \cdot \theta,$$

where  $\theta$  denotes the azimuth angle of the preceding vehicle with respect to the controlled vehicle coordinate system. The required change of a yaw rate ( $\Delta\gamma_{des}$ ) of the controlled vehicle should satisfy

$$D \cdot \frac{1}{2} (\gamma + \Delta\gamma_{des}) \cdot t_p = D \cdot \theta.$$

From the equation above,  $\Delta\gamma_{des}$  is derived as

$$\Delta\gamma_{des} = \frac{2\theta}{t_p} - \gamma.$$

The amount of a change of the steering angle is determined as

$$d\delta = K \cdot \Delta\gamma_{des} \cdot dt,$$

where  $dt$  denotes a period of control and  $K$  is a constant gain. In this study  $K$  is determined to be a value (=0.5 in this paper) which is minimizing  $J$ .

$$J = \int_0^\infty \varepsilon^2 dt,$$

where,  $\varepsilon$  denotes a tracking error. In a practical system,  $K$  will be tuned by road tests.

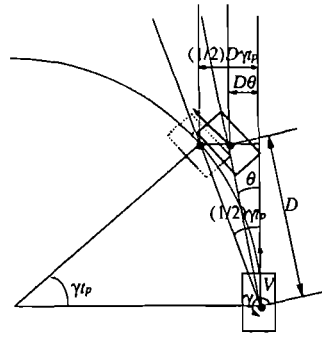


Fig.3. Algorithm 2

### 2.2.3. Algorithm 3

Algorithm 3 determines a steering angle in order that the controlled vehicle might track the trajectory of the preceding vehicle. By means of tracking the trajectory, the influence of a space between the two vehicles is excluded. In this algorithm, information of velocity, acceleration, yaw rate and side slip angle are necessary for calculation of a trajectory of the preceding vehicle. And they are used precise estimation of a future position of the controlled vehicle. This algorithm determines the steering angle not only by multiplying a gain by the change of yaw rate of the controlled vehicle required to reduce a future deviation to zero, which is the same manner as algorithm 2, but also by feeding back a present tracking error.

Figure 4 shows the variables used for the algorithm. The trajectory of the preceding vehicle with respect to the controlled vehicle coordinate system is calculated by transforming a detected relative position of the preceding vehicle, using transformation matrix given as follows:

$$T = \begin{pmatrix} \cos(\gamma dt) & \sin(\gamma dt) & -\{2(V dt / \gamma dt) \sin(\gamma dt / 2)\} \cos(\beta - \gamma dt / 2) \\ -\sin(\gamma dt) & \cos(\gamma dt) & -\{2(V dt / \gamma dt) \sin(\gamma dt / 2)\} \sin(\beta - \gamma dt / 2) \\ 0 & 0 & 1 \end{pmatrix}.$$

Assuming that the controlled vehicle travels at a constant yaw rate and a constant side slip angle, estimated a future lateral displacement in  $t_p$  [s] is given as

$$y_p = \left( V \cdot t_p + \frac{1}{2} a \cdot t_p^2 \right) \cdot \left( \frac{1}{2} \gamma \cdot t_p + \beta \right),$$

where  $t_p$  is defined as preview time (=0.5[s] in this paper). The required change of a yaw rate ( $\Delta\gamma_{des}$ ) should satisfy the following equation to reduce the future deviation to zero

$$\varepsilon = \left( V \cdot t_p + \frac{1}{2} a \cdot t_p^2 \right) \cdot \left\{ \frac{1}{2} (\gamma + \Delta\gamma_{des}) \cdot t_p + \beta \right\},$$

where  $\varepsilon$  denotes a relative lateral displacement of the point along the trajectory of the preceding vehicle  $V \cdot t_p + \frac{1}{2} a \cdot t_p^2$  [m] ahead with respect to the controlled vehicle. With the equation above,  $\Delta\gamma_{des}$  is given as

$$\Delta\gamma_{des} = \frac{2\varepsilon}{\left( V \cdot t_p + \frac{1}{2} a \cdot t_p^2 \right) t_p} - \frac{2\beta}{t_p} - \gamma.$$

The amount of a change of the steering angle is determined as

$$d\delta = (K_1 \cdot \Delta\gamma_{des} + K_2 \cdot \varepsilon) dt,$$

where  $\varepsilon$  denotes a present tracking error from the nearest point on the trajectory, and  $K_1$  and  $K_2$  are constant gains.  $K_1$  and  $K_2$  are determined by the same manner as algorithm 2.

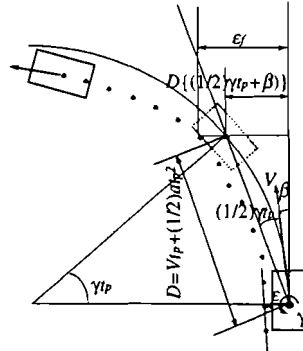


Fig.4 Algorithm 3

#### 2.2.4. Algorithm 4

Algorithm 4 determines a steering angle based on the azimuth angle  $\theta$ , see Figure 5, and a derivative of it as follows:

$$\delta = K(V, D) (\theta + C(V, D) \dot{\theta}),$$

where  $K(V, D)$  and  $C(V, D)$  are map functions of a vehicle speed and a space. They are calculated off-line using vehicle parameters. So this algorithm requires the information of vehicle parameters. The  $K(V, D)$  and  $C(V, D)$  are calculated for each 1[m/s] velocity step between 5 and 30[m/s], and for each 1[m] space step between 5 and 40[m]. And they are chosen according to a speed of the controlled vehicle and a space between the two vehicles at the point of time when the controlled vehicle is controlled.

The  $K(V, D)$  and  $C(V, D)$  at a speed of  $V$  and at a space of  $D$  are derived through the following process.

1. An ideal steering input of the following vehicle can be easily derived in the case where vehicle parameters of the preceding vehicle and the controlled vehicles are identical. The

ideal steering input of the controlled vehicle is given as  $\delta(t - D/V)$  with the steering input of the preceding vehicle  $\delta(t)$ .

2. An ideal tracking simulation at a velocity of  $V$ , at a space of  $D$  and at steering inputs of the preceding vehicle and the controlled vehicle of  $\delta(t)$  and  $\delta(t - D/V)$  respectively, is conducted to get values of  $\theta$  and  $\dot{\theta}$  at each time step. Coefficients of correlation between  $\delta(t - D/V)$  and  $\theta + C'\dot{\theta}$  are calculated for each 0.01 step of  $C'$  between -3.00 and 3.00, and  $C(V, D)$  is determined to be  $C'$  that makes the coefficient of correlation the closest to 1. This process derives the linear relation between  $\delta(t - D/V)$  and  $\theta + C(V, D)\dot{\theta}$ .

3. Since  $\delta(t - D/V)$  and  $\theta + C(V, D)\dot{\theta}$  have a linear relation,  $K'$  that satisfies the following equation can be obtained by the least squares method:

$$\delta(t - D/V) = K'(\theta + C(V, D)\dot{\theta}).$$

$K(V, D)$  is determined to be  $K'$ .

The following is confirmed by calculating  $K(V, D)$  and  $C(V, D)$  at various speeds, spaces, and steering inputs:  $K(V, D)$  and  $C(V, D)$  obtained by this process change according to the speed and the space, but they change relatively little according to the steering input. Figure 6 shows  $K(V, D)$  and  $C(V, D)$  of the vehicle model used in this paper (velocity=20[m/s], space=10~50[m] and space=20[m], velocity=5~30[m/s]).

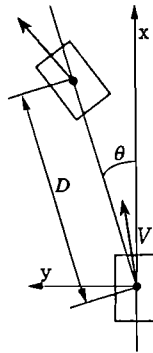


Fig.5 Algorithm 4

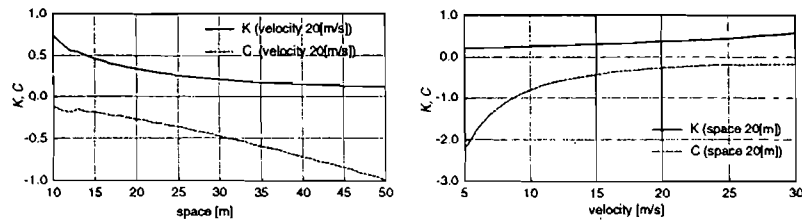


Fig.6  $K$  and  $C$  used in algorithm 4

### 2.2.5 Algorithm 5

Algorithm 5 determines a steering angle in order that the controlled vehicle might track a trajectory of the preceding vehicle, which is the similar manner as algorithm 3. Required lateral acceleration to track the trajectory is calculated on referring to the theory of sliding mode control, and the steering angle that generates the required lateral acceleration is derived from the equation of motion of a planar bicycle model. So this algorithm requires

the information of vehicle parameters as well as the state variables of vehicle dynamics.

Figure 7 shows the variables used for the algorithm. The trajectory of the preceding vehicle is calculated by the same manner as algorithm 3. Sliding surface is defined with a present tracking error ( $\varepsilon$ ) as follows:

$$S = c \int_0^t \varepsilon dt + \varepsilon ,$$

where  $c$  is a weighting coefficient ( $=0.4[s/l]$  in this paper). An input should satisfy

$$\dot{S} = -KS ,$$

that is

$$c\varepsilon + \dot{\varepsilon} + K \left( c \int_0^t \varepsilon dt + \varepsilon \right) = 0 , \quad (1)$$

where  $K$  is positive constant ( $=6.7[1/s]$  in this paper).  $K$  and  $c$  are determined by the same manner as algorithm 2. An average lateral velocity of the controlled vehicle from the present time to  $t_p[s]$  after is given as

$$\dot{y}_n = \left( V + \frac{1}{2} a \cdot t_p \right) \beta ,$$

where  $t_p$  is defined as preview time, which is  $0.5[s]$  in this paper. Estimated future tracking error in  $t_p[s]$  is given as

$$\varepsilon_p = \varepsilon_f - \int_0^{t_p} (\dot{y}_n + \ddot{y}_{des}) dt = \varepsilon_f - \dot{y}_{ntp} - \frac{1}{2} \ddot{y}_{des} t_p^2 ,$$

where  $\ddot{y}_{des}$  denotes desired lateral acceleration of the controlled vehicle, and  $\varepsilon_f$  expresses a relative lateral displacement of the point along the trajectory of the preceding vehicle  $V \cdot t_p + \frac{1}{2} a \cdot t_p^2 [m]$  ahead with respect to the controlled vehicle coordinate system.  $\dot{\varepsilon}$  is expressed as

$$\dot{\varepsilon} = \frac{\varepsilon_p - \varepsilon}{t_p} = \frac{\varepsilon_f - \dot{y}_{ntp} - \frac{1}{2} \ddot{y}_{des} t_p^2 - \varepsilon}{t_p} .$$

$\ddot{y}_{des}$  should satisfy the following equation to gratify the equation (1):

$$c\varepsilon + \frac{\varepsilon_f - \dot{y}_{ntp} - \frac{1}{2} \ddot{y}_{des} t_p^2 - \varepsilon}{t_p} + K \left( c \int_0^t \varepsilon dt + \varepsilon \right) = 0 .$$

From the equation above,  $\ddot{y}_{des}$  is derived as

$$\ddot{y}_{des} = \frac{2cK}{t_p} \int_0^t \varepsilon dt + \left\{ \frac{2(K+c)}{t_p} - \frac{2}{t_p^2} \right\} \varepsilon + \frac{2(\varepsilon_f - \dot{y}_{ntp})}{t_p^2} .$$

The steering angle to generate is determined through the following process. The equation of motion of a planar bicycle model with respect to the lateral movement is expressed as

$$m\ddot{y}_{des} = -(K_f + K_r)\beta - \frac{l_f K_f - l_r K_r}{V + \frac{1}{2} a \cdot t_p} \gamma + K_f \delta_{des} .$$

From the equation above, the steering angle is derived as

$$\delta_{des} = \frac{m\ddot{y}_{des}}{K_f} + \frac{K_f + K_r}{K_f} \beta + \frac{l_f K_f - l_r K_r}{(V + \frac{1}{2} a \cdot t_p) K_f} \gamma .$$

Since  $\delta_{des}$  is derived from the reverse calculation of the equation of motion with constant  $\beta$  and  $\gamma$ , however,  $\ddot{y}_{des}$  is not generated by the steering angle of  $\delta_{des}$ , in practice. So  $\delta_{des}$  requires the modifications to generate  $\ddot{y}_{des}$ . Estimated average lateral acceleration ( $\ddot{y}_{calc}$ ) generated at a steering angle of  $\delta_{des}$  from present time to  $t_p[s]$  after is derived from numerical



integration of the equation of motion.  $\delta_{des}$  is modified by the comparison of  $\ddot{y}_{calc}$  with  $\ddot{y}_{des}$  as follows:

$$\delta_{des} = \frac{\ddot{y}_{des}}{\ddot{y}_{calc}} \delta'_{des},$$

where  $\delta'_{des}$  represents the value of  $\delta_{des}$  before modified. In this study,  $\delta_{des}$  is modified two times by the method mentioned above.

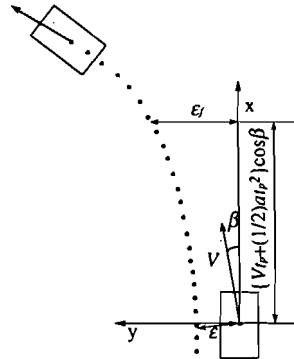


Fig.7 Algorithm 5

## 2.2 Vehicle-following simulations

### 2.2.1 Method of vehicle-following simulations

Vehicle-following simulations are conducted to evaluate the tracking accuracy based on the control algorithms. A planar bicycle model with 3 DOFs (the longitudinal, the lateral and the yaw movement) is used in the simulations. Calculation is conducted at 0.01[s] step, and a period of the control is 0.05[s]. Figure 8 shows the supposed trajectory of the preceding vehicle. The minimum trajectory radius of curvature at a speed of 20[m/s] is 105[m], and the lateral acceleration at that point is 0.4G. In conducting simulations, three kinds of conditions are considered as follows.

- Vehicle following at a constant speed and space
  - simulation 1-1: velocity is 20[m/s]; and space is 20[m].
  - simulation 1-2: velocity is 10[m/s], and space is 20[m].
- Vehicle following at a changing speed or space
  - simulation 2-1: velocity is  $20+3\sin(t/2)$ [m/s], space is 20[m].
  - simulation 2-2: velocity is 20[m/s], and space is  $20+6\sin(t/2)$ [m].
- Vehicle following with different parameters of vehicle from those assumed in the control algorithms
  - simulation 3-1: mass is  $1.3m$ , and inertia is  $1.3I$  ( $m$  and  $I$  are values assumed in the control algorithms.).
  - simulation 3-2: total cornering power of front tires is  $0.7K_f$ , and total cornering power of rear tires is  $0.7K_r$  ( $K_f$  and  $K_r$  are assumed values in the control algorithms.).

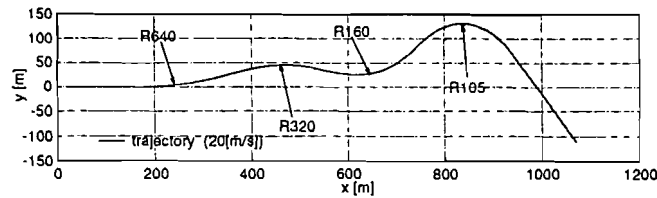


Fig .8 Trajectory of the preceding vehicle

### 2.2.2 Simulation results

Simulation results are shown in Figure 9 and 10, and table 2 shows maximum tracking errors in each of the simulations. A tracking error of the CG of the controlled vehicle from the trajectory of the CG of the preceding vehicle is shown as results. When CG of the controlled vehicle deviates to the right from the trajectory of the preceding vehicle, the error has a positive value.

Under all conditions, control algorithm 3 and 5 realize accurate tracking, since both algorithms utilize full state variables shown in table 1. Algorithm 2, which utilizes the information of velocity and yaw rate, does not perform accurate tracking. Therefore, it is fair to say that side slip angle is the essential information for accurate tracking in the lateral direction. Acceleration is influential only when a speed is changing. Considering the simulation results of algorithm 3, it is also fair to say that measurement of state variables of vehicle dynamics (velocity, acceleration, yaw rate and side slip angle), in spite of the lack of the information of vehicle parameters, enables fine tracking to some extent.

Simulation results also indicate that control algorithm 4 realizes accurate tracking on the restricted condition of a short headway time (about 1[s] is desirable) and a constant spacing distance, which means that the longitudinal control is restricted for implementing the lateral control. The tracking performance obtained by control algorithm 4 is subject to the influence of parameter errors and disturbances.

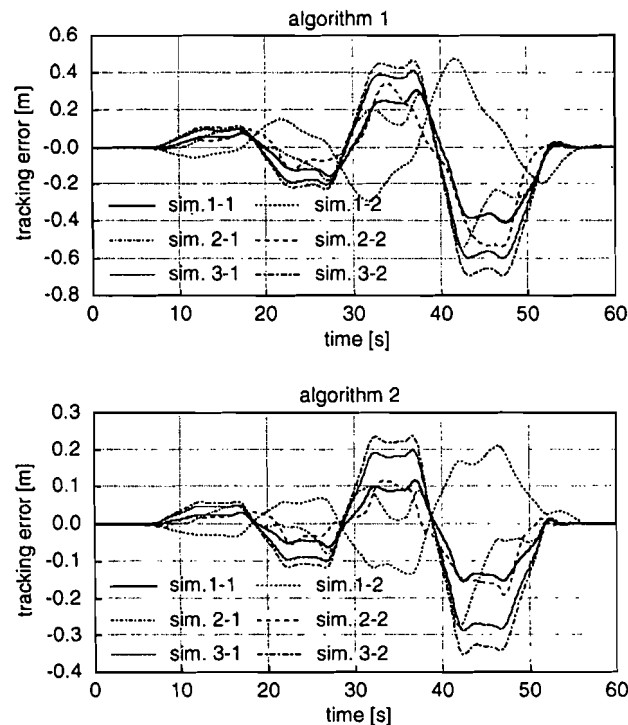


Fig. 9 Simulation results (algorithm 1 and 2)

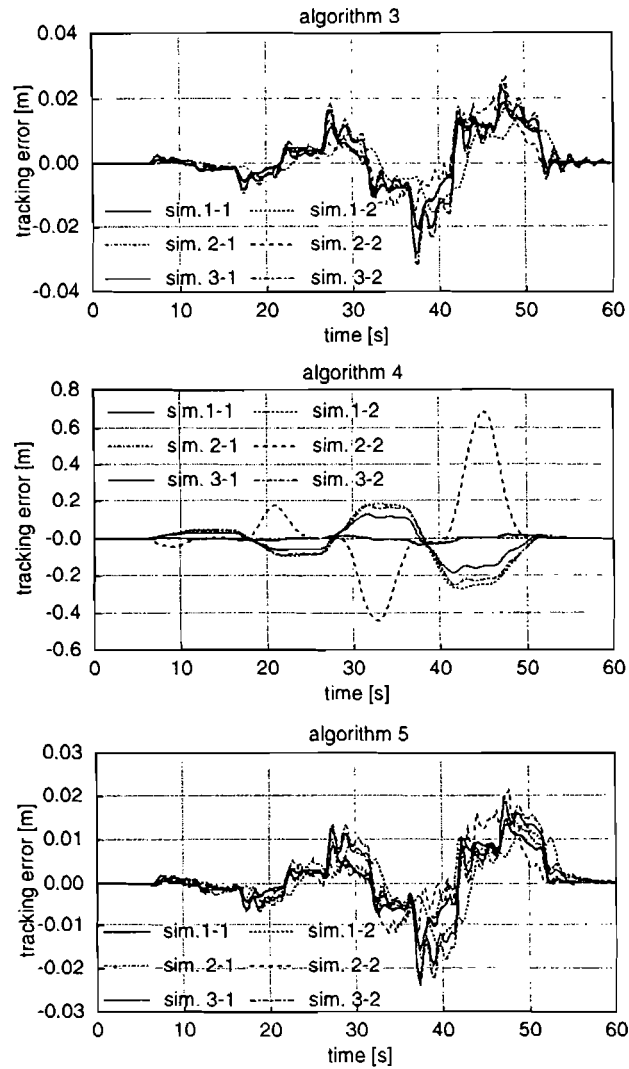


Fig. 10 Simulation results (algorithm 3, 4 and 5)

Table 2 Maximum tracking errors

| control<br>algorithm | constant speed and space      |                               | changing speed and space                        |   | different vehicle parameters                             |   |
|----------------------|-------------------------------|-------------------------------|---|---|--|---|
|                      | simulation 1-1                | simulation 1-2                | simulation 2-1                                  | simulation 2-2                                  | simulation 3-1   | simulation 3-2  |
|                      | velocity20[m/s]<br>space20[m] | velocity10[m/s]<br>space20[m] | velocity<br>$20+3\sin(t/2)$ [m/s]<br>space20[m] | velocity20[m/s]<br>space<br>$20+6\sin(t/s)$ [m] | mass properties<br>are different<br>vel.20[m/s] sp.20[m] | cornering powers<br>are different<br>vel.20[m/s] sp.20[m] |
| 1                    | 0.4[m]                        | 0.5[m]                        | 0.5[m]  | 0.5[m]  | 0.6[m]   | 0.7[m]  |
| 2                    | 0.16[m]                       | 0.2[m]                        | 0.3[m]  | 0.2[m]  | 0.3[m]   | 0.35[m]   |
| 3                    | 0.02[m]                       | 0.015[m]                      | 0.02[m]   | 0.025[m]  | 0.03[m]  | 0.03[m]   |
| 4                    | 0.03[m]                       | 0.3[m]                        | 0.05[m]   | 0.7[m]  | 0.2[m]   | 0.25[m]   |
| 5                    | 0.015[m]                      | 0.015[m]                      | 0.015[m]  | 0.02[m]   | 0.02[m]  | 0.02[m]   |

### 3 EXPERIMENTAL STUDY

Road tests using two vehicles are carried out for the purpose of confirming the validity of the simulation study. Three things are confirmed — validity of simulation model, the influence of information of side slip angle, and the robustness to influence of a change of a speed and space.

Control algorithm 3 is used in the road tests because of the accuracy and simplicity of the algorithm. At the road tests, gains of the algorithm are the same values as those of the simulation study. It should be noted that, for stability consideration, preview time is  $V/D$ , which is different from that of the simulation study.

#### 3.1 Experimental setup

Experimental vehicles comprise two sedan-type cars, preceding-vehicle-detection system, actuator system, sensing system and computers. The preceding vehicle is controlled by a human driver, and longitudinal control of the controlled car is implemented by a human driver.

The preceding-vehicle-detection system consists of a scanning laser radar and corner-cube reflectors. The laser-scanning-station method is adopted for the detection[17]. The scanning laser radar is installed on roof of the controlled vehicle, see Figure 11. Corner-cube reflectors attached on the preceding vehicle, see Figure 12. This system detects a relative position of the preceding vehicle with respect to the controlled vehicle every 25[ms]. Detected lateral position error is less than 0.04[m] at a space of 10[m], and 0.05[m] at a space of 20[m]. Detected longitudinal position error is less than 0.15[m] at a space of 10[m], and 0.3[m] at a space of 20[m].

The actuator system is composed of an AC servomotor, reduction gears and a electromagnetic clutch. This system turns a steering handle of the controlled vehicle according to the desired steering angle calculated by a computer. Dynamic density is 0.85[deg] at the steering handle.

The sensing system measures state variables of velocity and yaw rate. Side slip angle is estimated by an observer.

The computer (CPU: Intel 486DX4 100MHz) processes signals from the sensors and the scanning laser radar and calculates the trajectory of the preceding vehicle, the tracking error, and the desired steering angle of the controlled vehicle.

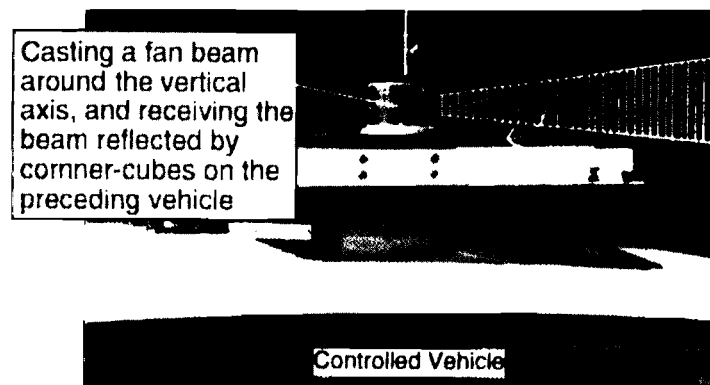


Fig. 11 Scanning laser radar on the controlled vehicle

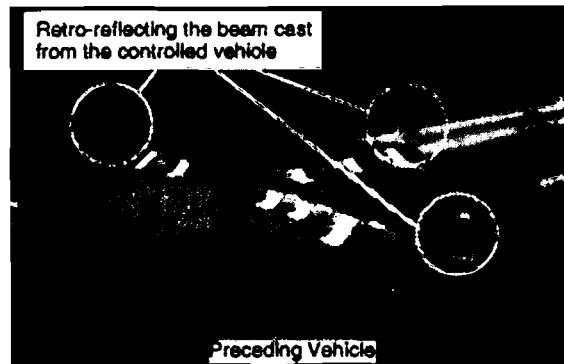


Fig. 12 Corner-cube reflectors on the preceding vehicle

## 3.2 Road tests

### 3.2.1 Method of road tests

To confirm the validity of the simulation model, characteristic of step responses with 1[m] of initial tracking error is investigated and compared with simulation results. To confirm the influence of information of side slip angle, tracking accuracy at a circling maneuver (road radius of curvature; 180[m]) is investigated. The tracking accuracy with the information of side slip angle is compared with that without the information. Those two road tests are conducted under the following four conditions.

- velocity is 5[m/s], and space is 10[m].
- velocity is 10[m/s], and space is 15[m].
- velocity is 15[m/s], and space is 15[m].
- velocity is 20[m/s], and space is 20[m].

To confirm the robustness to the influence of a change of a speed and space, tracking accuracy at a circling maneuver (road radius of curvature; 180[m]) under the following two conditions is investigated.

- velocity is changing between 10[m/s] and 20[m/s], and space 15[m].
- velocity of the preceding vehicle is 15[m/s], and space is changing between 10[m] and 20[m].

### 3.2.2 Results of road tests

Figure 13 shows the experimental results and simulation results of step response. A tracking error of the CG of the controlled vehicle from the trajectory of the CG of the preceding vehicle is shown as results. When CG of the controlled vehicle deviate to the right from the trajectory of the preceding vehicle, the error has a positive value. The simulation results correspond well with the experimental results under all conditions, which indicates that the simulation model correctly represents the experimental vehicle.

Figure 14 shows the experimental results of a circling maneuver at a constant speed and space. There is a difference between the results of tracking with information of side slip angle and those without the information. As to the results of 5[m/s] and 10[m/s], offsets of the tracking error are observed in the tracking without information of side slip angle. As to the result of 15[m/s], the tracking errors of both tracking are similar. The reason for the similarity is because side slip angle at 15[m/s] is relatively small in comparison with that at the other velocities. Those results indicate that lateral control using the information of side slip angle effectively reduces the offset of a tracking error. They also indicates that tracking

errors of tracking with information of side slip angle are less than 5[cm] under all conditions.

Figure 15 shows the experimental results of a circling maneuver at a changing speed or space. Tracking errors are oscillatory in comparison with results of a constant speed and space shown in Figure 14. But the tracking errors are not divergent and are less than 10[cm] under both conditions. Those results indicate that the vehicle-following control algorithm has the robustness to the influence of a change of a speed and space.

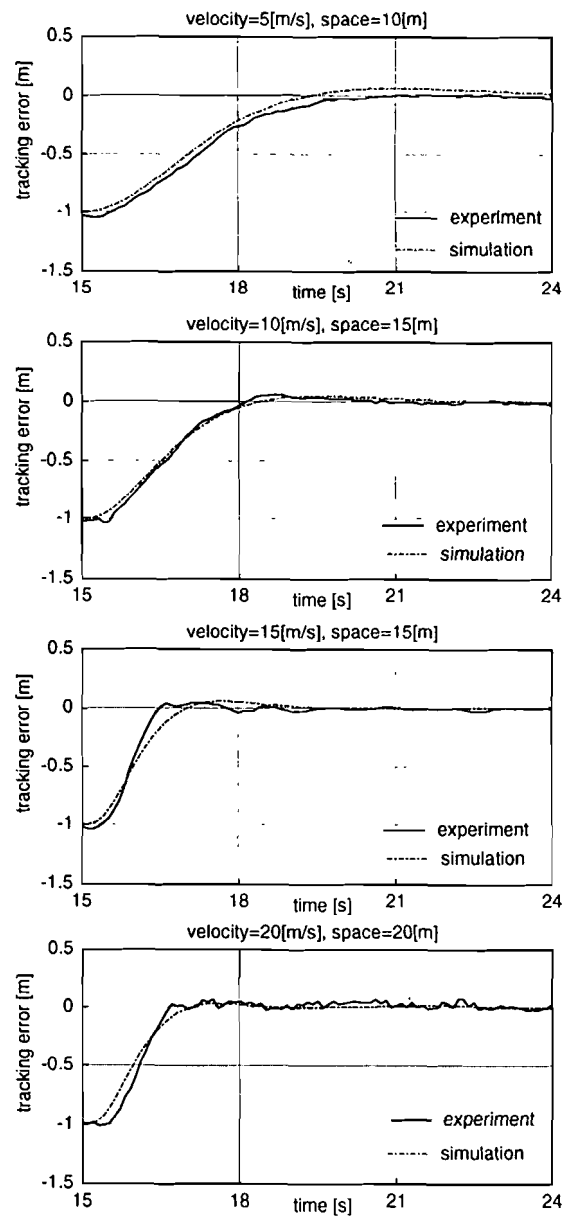


Fig. 13 Experimental and simulation results of step responses

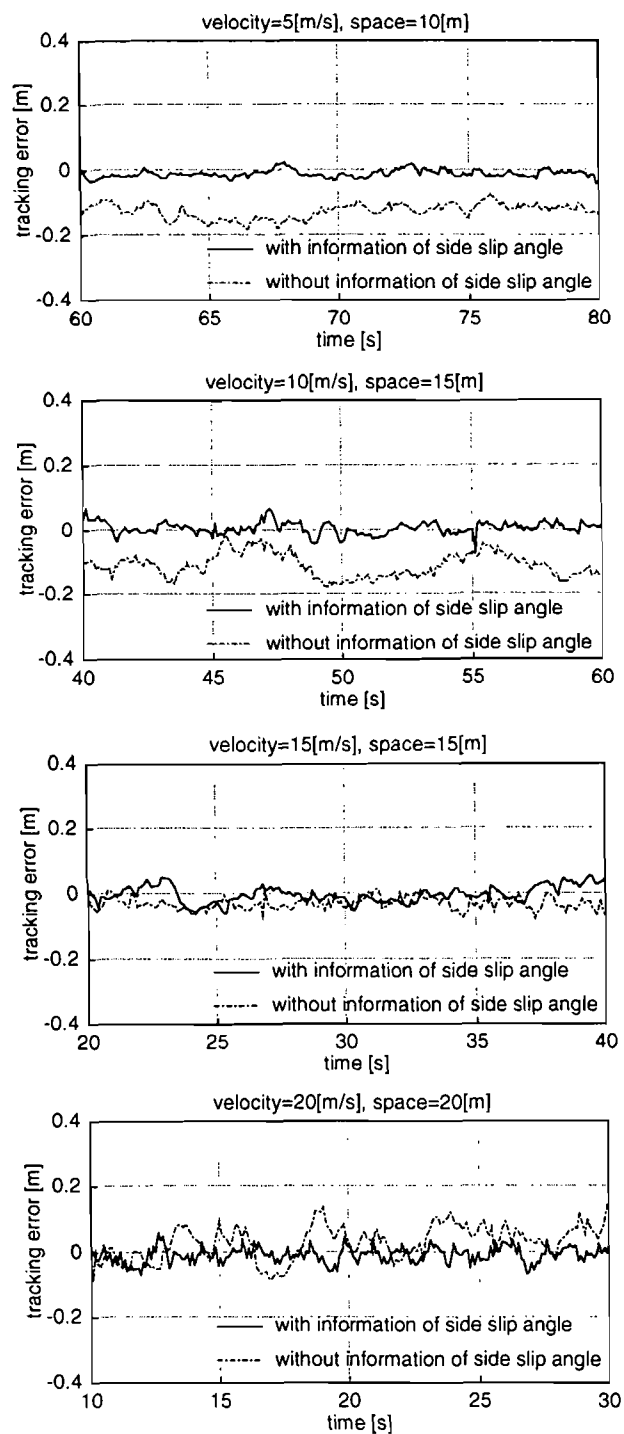


Fig. 14 Experimental results of circling maneuver at a constant speed and space

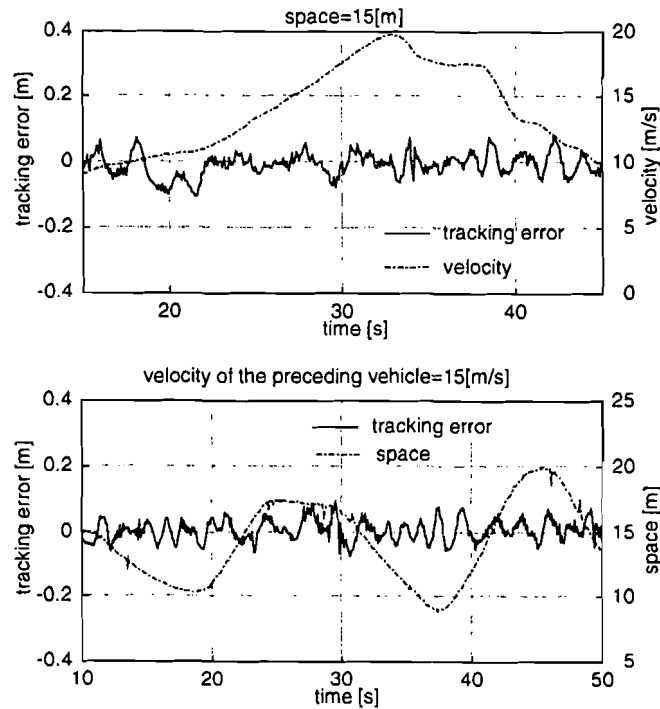


Fig. 15 Experimental results of circling maneuver at a changing speed and space

#### 4 CONCLUSIONS

In this paper, lateral vehicle-following control is investigated by the simulations and the experiments. Five kinds of lateral control algorithms are proposed and compared by the simulations. The comparison of the simulation results indicates the relationship between the information for lateral control and the tracking accuracy. The validity of the simulations are confirmed by comparison between experimental results and simulation results of step responses. It is verified by the simulations and the experiments that side slip angle is the essential information for accurate tracking. It is also verified that the controller little dependent on vehicle parameters can perform accurate tracking and that the controller has the robustness to the influence of a change of a speed and space.

The control algorithms proposed in this paper can be also applied to road-following control, since the position of the road center instead of the position of the preceding vehicle is the target in the road-following control system.

In this study, non-linearity and uncertainty of the system, e.g. tire force saturation, lag of side tire force, lags of actuators, errors of sensors are not taken into consideration for designing the control algorithms. Designing controllers with considering those influence is thought to be future works.



## REFERENCES

1. T. Fujioka, M. Omae, : *Control Algorithms for Lateral Platooning*, Proceedings of the Third World Congress on Intelligent Transport System, (1996).
2. U.N.Petersen, A. Ruekgauer, W.O. Schiehlen, : *Lateral Control of a Convoy Vehicle System*, Proceedings of 14th IAVSD-Symposium, (1996), pp. 519-532.
3. Pascal Daviet, Michel Parent, : *Longitudinal and Lateral Servoing of Vehicle in a Platoon*, Proceedings of the 1996 IEEE Intelligent Vehicles Symposium, (1996), pp. 41-46.
4. T. Fujioka, K. Suzuki, : *Control of Longitudinal and Lateral Platoon Using Sliding Control*, Vehicle System Dynamics, Vol.23, No.8, (1994), pp.647-664.
5. JUERGEN GULDNER, HAN-SHUE TAN, SATYAJIT PATWARDHAN, : *Analysis of Automatic Steering Control for Highway Vehicles with Look-down Lateral Reference System*, Vehicle System Dynamics, Vol.26, No.4, (1996), pp. 243-269.
6. Hideaki Inoue, Hiroshi Mouri, Hiroshi Sato, Akira Asaoka, Satoshi Ueda, : *Technologies of Nissan's AHS Test Vehicle*, ITS World Congress 96, (1996).
7. Ken-ich YOSHIMOTO, Hideki OGAWA, Hiroshi KUBOTA, : *A Course Tracking Control Algorithm using Visual Information*, Proceeding of the International Symposium on Advanced Vehicle Control 1996, Vol.2, (1996), pp. 1305-1320.
8. Akihide Tachibana, Keiji Aoki, Hiroshi Tominaga, : *The Lateral Control Strategy on Magnetic Nail based AHS Lane*, ITS World Congress 96, (1996).
9. Saied Mammari, :  *$H_{\infty}$  Robust Automatic Steering of a Vehicle*, Proceedings of the 1996 IEEE Intelligent Vehicles Symposium, (1996), pp. 19-24.
10. Soon-Hwan Moon, Chai-Won Kim, Min-Hong Han, : *Navigation Control for an Autonomous Road Vehicle using Neural Network*, Proceedings of the Third World Congress on Intelligent Transport System, (1996).
11. Ty A. Lasky, Bahram Ravani, : *Lateral Vehicle Control for AHS using a Laser Sensor*, Proceedings of the Second World Congress on Intelligent Transport System, (1995), pp. 1082-1087.
12. Umit Ozguner, Konur A. Unyelioglu, Cem Hatipoglu, Franz Kautz, : *Design of a Lateral Controller for Cooperative Vehicle Systems*, SAE Transaction 1995, Paper No. 950474, (1995), pp. 27-34.
13. Hung Pham, Karl Hedrick, Masayoshi Tomizuka, : *Autonomous Steering and Cruise Control of Automobiles via Sliding Mode Control*, Proceeding of the International Symposium on Advanced Vehicle Control 1994, Paper No. 9438673, (1994), pp. 444-448.
14. DIRK E. SMITH, JOHN M. STARKEY, : *Effects of Model Complexity on the Performance of Automated Vehicle Steering Controllers: Controller Development and Evaluation*, Vehicle System Dynamics, Vol.23, No.8, (1994), pp. 627-645.
15. Huei Peng, Weibin Zhang, Steven Shladover, Masayoshi Tomizuka, : *Magnetic-Marker-Based Lane Keeping: A Robustness Experimental Study*, SAE Transaction 1993, SAE Paper No. 930556, (1993), pp. 750-755.
16. M. TOMIZUKA, J. K. HEDRICK, : *AUTOMATED VEHICLE CONTROL FOR IVHS SYSTEMS*, The1993 IFAC Conference, (1993).
17. Toshihiro Tsumura, Hiroshi Okubo, Nobuo Komatsu, : *New Approaches for a Fully Optical Positioning, Guidance, Navigation and Communication System for Ground Vehicles*, Proceedings of the Second World Congress on Intelligent Transport System, (1995), pp. 628-634.